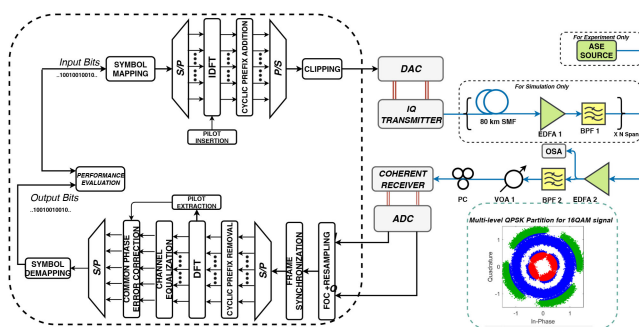


Pilot-Free Common Phase Error Estimation for CO-OFDM With Improved Spectral Efficiency

Volume 11, Number 6, December 2019

Lakshmi Narayanan Venkatasubramani
Anirudh Vijay
Deepa Venkitesh
R. David Koilpillai, *Member, IEEE*



DOI: 10.1109/JPHOT.2019.2949637

Pilot-Free Common Phase Error Estimation for CO-OFDM With Improved Spectral Efficiency

Lakshmi Narayanan Venkatasubramani , Anirudh Vijay, Deepa Venkitesh, and R. David Koilpillai, *Member, IEEE*

Department of Electrical Engineering, Indian Institute of Technology Madras, Chennai 600036, India

DOI:10.1109/JPHOT.2019.2949637

This work is licensed under a Creative Commons Attribution 4.0 License. For more information, see <https://creativecommons.org/licenses/by/4.0/>

Manuscript received September 21, 2019; revised October 18, 2019; accepted October 20, 2019. Date of publication October 25, 2019; date of current version November 26, 2019. This work was supported in part by the Office of the Principal Scientific Adviser, Govt. of India, in part by the Department of Science and Technology, Govt. of India, in part by the Ministry of Electronics and Information Technology, Govt. of India, and in part by the Ministry of Human Resource Development, Govt. of India. Corresponding author: Lakshmi Narayanan Venkatasubramani; Deepa Venkitesh (e-mail: ee14d402@ee.iitm.ac.in; deepa@ee.iitm.ac.in).

Abstract: We propose an improved pilot free phase noise mitigation algorithm for CO-OFDM systems using weighted multi-level QPSK partitioning and Kalman filtering. Through extensive Monte Carlo simulations, we demonstrate an improvement in spectral efficiency of >6% in case of 200 Gbps single channel and 1 Tbps multi channel 16QAM CO-OFDM transmission with blind carrier phase estimation. We also experimentally demonstrate the performance of the proposed algorithm against the standard pilot aided algorithm for the transmission of 120 Gbps 16QAM CO-OFDM at different noise levels.

Index Terms: Coherent optical OFDM, phase noise, common phase error, Kalman filter.

1. Introduction

Several applications such as 5G wireless, cloud computing and virtual reality demand the physical layer to process signals at very high speeds. The transponder bit rates can be increased by employing high symbol rate transmission by deploying electrical domain frequency multiplexing for realizing higher bit rate DACs and ADCs [1]. In such multiplexing methods, the entire signal frequency band is split into smaller segments and each segment is independently operated using a low-speed DACs/ADCs. In such scheme where frequency interleaving is involved, a multi-carrier scheme would be preferred over a single carrier scheme. Coherent optical OFDM (CO-OFDM) is one such multi-carrier scheme that is comprehensively investigated in optical communication systems as an alternate to Nyquist pulse shaped single carrier transmission for >Terabit/s transmission and inelastic optical networks [2]. CO-OFDM also has extreme tolerance to linear fiber impairments such as chromatic dispersion and polarization mode dispersion and hence enables simple equalization [3].

However, due to the longer symbol duration (T_s), the CO-OFDM system is more susceptible to phase noise due to laser linewidth ($\frac{\Delta\nu}{2}$) and hence suffers performance degradation due to common phase error (CPE) and inter carrier interference (ICI) [4]. Pilot aided (PA) CPE estimation methods have been proposed in the past [5], [6], where pilot symbols are used to estimate the CPE. Such pilot aided methods incur loss of spectral efficiency since a fraction of potential information

subcarriers are used as pilot subcarriers. Non-pilot aided zero-overhead CPE estimations were proposed in [7], [8] by using higher order statistics and decision directed (DD) iterative algorithms. These methods use all subcarriers for the estimation process and are computationally expensive. For instance, [7] estimated the complexity of the DD algorithm to be almost 28% additional compared to the conventional pilot aided algorithm. In addition, DD-CPE algorithms inherit error propagation when the initialization is erroneous or when the laser linewidth is large (>100 KHz) [7]. In [9], the authors have proposed CPE based on simplified extended Kalman filtering but again use DD estimation in a blind mode.

In this paper, we propose a novel blind CPE estimation stage followed by a linear Kalman filter fourth power algorithm (K4P algorithm) for CPE prediction and compensation in CO-OFDM system. We demonstrate its capability to tolerate higher normalized linewidth ($\Delta\nu T_s$) and compare its performance with the PA algorithm [5] using extensive Monte Carlo simulations. The blind estimates are obtained using two-level weighted QPSK partitioning of square MQAM constellations. For a 16QAM, 32 GBd, CO-OFDM system, we evaluate and compare the performance of K4P algorithm with PA scheme for two scenarios: (a) back-to-back (B2B) configuration to evaluate the OSNR penalty (to achieve a BER of 1×10^{-3}) incurred by the proposed algorithm (b) transmission of PM-16QAM, CO-OFDM signal over 1600 km of uncompensated standard single mode fiber (SSMF) at for an information rate of 200 Gbps and 1 Tbps. We quantify the improvement in spectral efficiency and reach extension for different values of normalized linewidth for 16QAM-OFDM modulation. We also experimentally demonstrate the performance of the K4P algorithm for 120 Gbps 16QAM CO-OFDM at various OSNRs.

The paper is organized as follows: Section 2 presents details of theory and modeling of the CO-OFDM in presence of phase noise along with description of the proposed algorithm and its complexity analysis, Section 3 & 4 describes the Monte Carlo simulation details of CO-OFDM with associated impairments followed by numerical results and Section 5 describes the experimental setup and associated results.

2. Theory & Model

2.1 Phase Noise Model in CO-OFDM

In the presence of laser phase noise and additive white Gaussian noise (AWGN), the received polarization multiplexed CO-OFDM signal- for an optical flat channel can be expressed in terms of the transmitted symbols [9] in the frequency domain as

$$Y_m(k) = X_m(k)I_m(0) + ICI_m(k) + W_m(k) \quad (1)$$

where $k = 1, 2, \dots, N_{FFT}$ and N_{FFT} is the number of subcarriers; $Y_m(k)$, $X_m(k)$, $ICI_m(k)$ and $W_m(k)$ represent the received signal, transmitted signal, Inter Carrier Interference (ICI) and AWGN terms respectively in the k th sub-carrier of the m th OFDM symbol. The ICI component due to phase noise is described as

$$ICI_m(k) = \sum_{l=0, l \neq k}^{N_{FFT}-1} X_m(l)I_m(l-k), \quad (2)$$

with

$$I_m(p) = \frac{1}{N_{FFT}} \sum_{n=0}^{N_{FFT}-1} e^{j\left[\frac{2\pi p n}{N_{FFT}} + \phi_m(n)\right]} \quad (3)$$

where $I_m(0)$ is the common phase error (CPE) factor given as $I_m(0) \approx \exp(j\phi(m))$ and $\phi(m)$ is the CPE across the subcarriers of the m th OFDM symbol given as

$$\phi(m) = \arg \left\{ \frac{1}{N_{FFT}} \sum_{n=0}^{N_{FFT}-1} e^{j\phi_m(n)} \right\}. \quad (4)$$

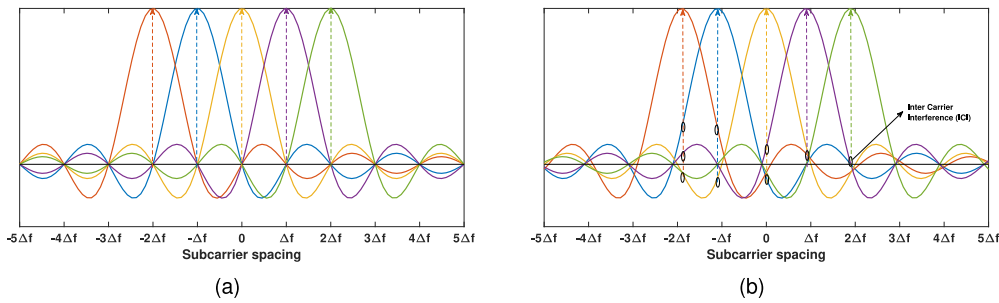


Fig. 1. Illustration of inter carrier interference in OFDM systems. Fig. (a) is used as reference (uncorrupted by phase noise). Fig. (b) shows overlapping frequency components indicate the effect of ICI.

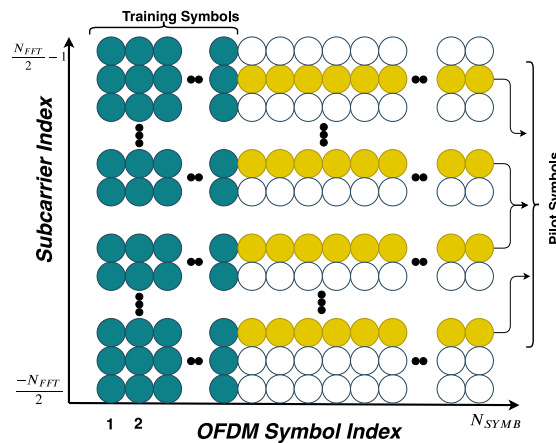


Fig. 2. Time and frequency distribution of OFDM symbols including the training symbols and pilot symbols.

This phase can be modeled as a Wiener process, $\phi(m) = \phi(m - 1) + \Delta\phi(m)$ where $\Delta\phi(m)$ is a Gaussian random variable with zero mean and variance $2\pi\Delta\nu T_s$. Fig. 1(a) shows the frequency domain picture where the subcarriers are not corrupted by phase noise. Fig. 1(b) shows the case where there is a common phase error among the subcarriers and inter carrier interference which result in the loss of orthogonality. The neighbouring subcarriers in this case have finite, non-zero contribution to the subcarrier of interest, which is indicated as open ellipses in the same figure. We now proceed to discuss ways to estimate and correct the common phase error.

2.2 Pilot Aided CPE Estimation

Pilot aided carrier phase estimation is one of the most widely used phase noise correction technique both in wireless and optical transmission schemes for OFDM systems. Several subcarrier are loaded with known symbols, known at both transmitter and receiver, which are designated as pilot symbols. Fig. 2 shows the pictorial representation of such scheme where, the dots in yellow show the pilot symbols interspersed across the subcarriers. The blue dots indicate the training symbols, which is used for channel estimation and equalization. The required number of pilot tones are decided by the laser linewidth. In this method these pilots are used at the receiver to estimate the CPE as [7], [8]

$$\Phi(m) = \arg \left(\frac{1}{N_p} \sum_{j=1}^{N_p} \frac{Y_m(j)X_m^*(j)}{|Y_m(j)X_m^*(j)|} \right) \quad (5)$$

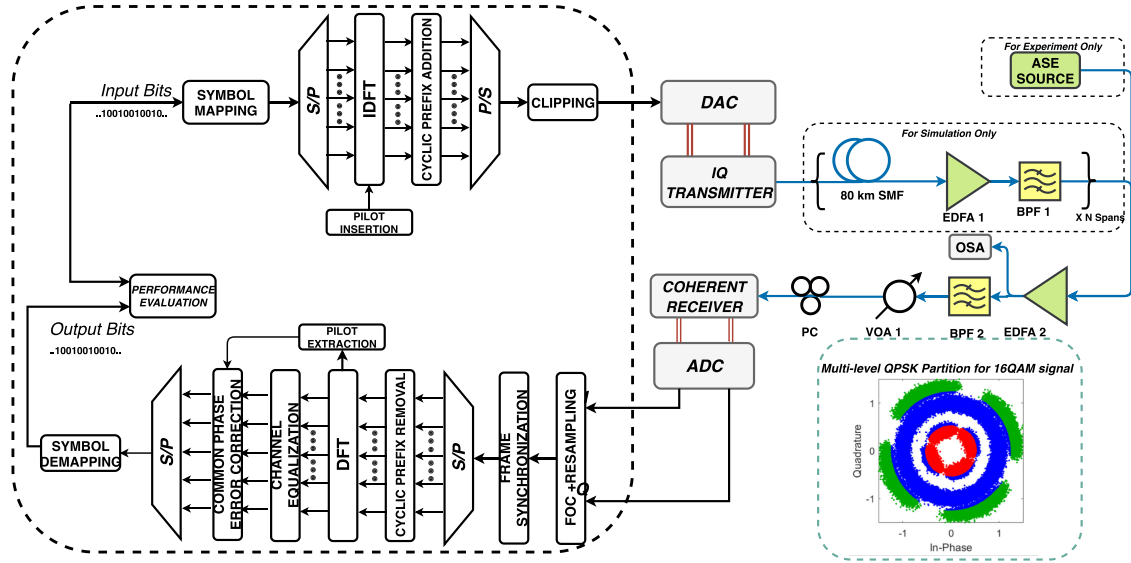


Fig. 3. Schematic of the simulation & experimental setup to perform long haul transmission/emulation. For B2B case, $N_{SPA} = 0$. (Inset: Multi-level QPSK partitioning of 16QAM points showing inner (red) and outer (green) points).

where, N_p is the number of pilots used. Use of such pilot symbols by substituting the actual information that needs to be transmitted, occupies additional bandwidth and will also reduce the effective information rate of transmission.

2.3 Pilot-Free K4P Algorithm

We propose an alternate OFDM frame structure that is devoid of pilot tones. The proposed structure has one training symbol (or a preamble) for the channel equalization and is followed by data symbols. Kalman filtering is proposed to estimate the CPE recursively for the OFDM symbols in the received frame in the following manner. The a priori ($\phi_{m|m-1}$) and the a posteriori (ϕ_m) CPE estimates of the k th OFDM symbol in the Kalman filter equation are initialized by phase estimate from the training symbol and zero respectively. The entire symbol is first rotated by the a priori phase estimate to prevent any phase slip due to the blind estimation. In any square MQAM modulation, the outer most and the inner most constellations points resembles QPSK modulated symbols, whose phase angles are $(2n + 1)\frac{\pi}{4}$, where $n = 0, 1, 2, 3$. In such square MQAM baseband modulated data, a multi-level QPSK partitioning [10] is performed to extract the outermost and the innermost QPSK points from the constellation. Inset of Fig. 3 shows such partitioning for 16QAM modulated data. These samples are then raised to the fourth power to estimate (in blind sense) the mean rotation angle θ_m^{in} and θ_m^{out} for each sets independently.

The rotation angle estimates are accurate when the total number of filled subcarriers N_{filled} is large and there are sufficient subcarriers carrying inner and outer constellation points. The rotation angle estimate θ_m^w , is the weighted average of the individual estimates: the weights γ and $(1 - \gamma)$ are in the ratio of the amplitude of ideal outer to that of ideal inner constellation points ($\gamma = 0.75$ for 16QAM, $\gamma = 0.875$ for 64QAM). The Kalman filter prediction (assuming Wiener process) and measurement update steps are given by

$$\theta_m^w = \gamma \theta_m^{out} + (1 - \gamma) \theta_m^{in} + \hat{\phi}_{m|m-1} \quad (6)$$

$$\hat{\phi}_{m+1|m} = \hat{\phi}_{m|m-1} + K_m (\theta_m^w - \hat{\phi}_{m|m-1}), \quad (7)$$

where K_m is the Kalman gain and the error covariance (P_m) prediction and update are recursively updated using standard Kalman filter equations [11]. The measurement noise covariance and

TABLE 1

Complexity Analysis of Proposed K4P Algorithm CM: Complex multiplication, RM: Real Multiplication

Process	Step	# of Operations
Mean angle of outer constellation points	$\theta_m^{out} = f(\mathbf{R}_m^{out})$	$6N_{FFT}\Lambda$ (CM)
Mean angle of inner constellation points	$\theta_m^{in} = f(\mathbf{R}_m^{in})$	$6N_{FFT}\Lambda$ (CM)
Prediction	$\theta_m^w = \gamma\theta_m^{out} + (1-\gamma)\theta_m^{out} + \hat{\phi}_{m m-1}$	2 (RM)
Measurement noise covariance update	$R_{E,m} = P_{m m-1} + R$	0
Kalman gain update	$K_m = P_{m m-1}/R_{E,m}$	1 (RM)
Measurement update	$\hat{\phi}_{m+1 m} = \hat{\phi}_{m m-1} + K_m(\theta_m^w - \hat{\phi}_{m m-1})$	1 (RM)
Error covariance update	$P_{m+1 m} = P_{m m-1}(1-K_m) + Q$	1 (RM)
CPE correction	$Y_m(k) = \mathbf{R}_m(k)\exp(-j\hat{\phi}_{m+1 m})$	N_{FFT} (CM)
Total		$\approx (12\Lambda + 1)N_{FFT}$ (CM)

process noise covariance are empirically optimized for a robust tracking based on the optical signal to noise ratio (OSNR) and linewidth ($\frac{\Delta\nu}{2}$) respectively. Typically the process noise covariance can be approximated to $2\pi(\Delta\nu)T_s$ and the measurement noise can be estimated based on the OSNR of the received signal (as measured from the optical spectrum analyzer). In order to prove the efficacy of this algorithm, we compare its performance with a standard PA scheme with different numbers of pilot subcarriers (PA-x, x: number of pilot subcarriers) and the results are discussed in Section 3. The key benefit of using the pilot-free algorithm is its increased spectral efficiency (SE), which is defined as the amount of information transmitted per unit bandwidth. In pilot aided transmission, the bandwidth is used by both the information and pilots symbols. But in the pilot-free transmission, the bandwidth is occupied only by the information symbol and hence the SE is increased. For a given occupied spectrum for the data, we do not expect an improvement in BER. The blind algorithm enables us to use more number of data subcarriers and thus improve the spectral efficiency.

2.4 Computational Complexity

In order to estimate the computational complexity of the proposed K4P algorithm, we evaluate the number of real multiplications (RM) and complex multiplications (CM) involved. Table 1 shows the number of operations involved in the K4P algorithm. Single real division is treated as a single real multiplication. In this analysis, Λ is the factor defined as the ratio of outermost QPSK like constellation points to the total number of constellation points in any modulation format, its value is 1 for QPSK, 0.25 for 16QAM. Total number of complex multiplications involved per polarization in case of our proposed K4P algorithm is $\approx (12\Lambda + 1)N_{FFT}$, ($N_{FFT} \approx 128$), which is only linear in N_{FFT} . In the case of pilot aided scheme, the computational complexity is only linear in the number of pilots used ($N_p \approx 8$) and hence it is less computational complex compared to the proposed pilot-free algorithm. However, in spite of having an increased computational complexity, pilot-free algorithm works without incurring any performance degradation.

3. Simulation Setup

The schematic of the simulation setup is shown in the Fig. 3. A 32 GBd OFDM signal is generated by digitally modulating data using IFFT operation onto $N_{FFT} = 128$ subcarriers. The data and pilot subcarriers (only for PA case) are respectively loaded with 16QAM samples from PRBS-15 bit stream and QPSK samples, amounting to a total of N_{filled} subcarriers. Cyclic prefix of length $N_{CP} = 3$ is added to each OFDM symbol to compensate for polarization mode dispersion. The OFDM frame contains a training symbol (preamble) used for channel estimation and equalization and followed by $2^9 - 1$ symbols. An optimized clipping ratio of 4 was used. The signal is then modulated on an optical carrier, in each polarization, at 1550 nm (linewidth = $\frac{\Delta\nu}{2}$) using an IQ modulator. Modulated optical signal then numerically transmitted through various spans of single mode fiber and the link loss is compensated using mid span amplifiers. The optical signal is then coherently detected,

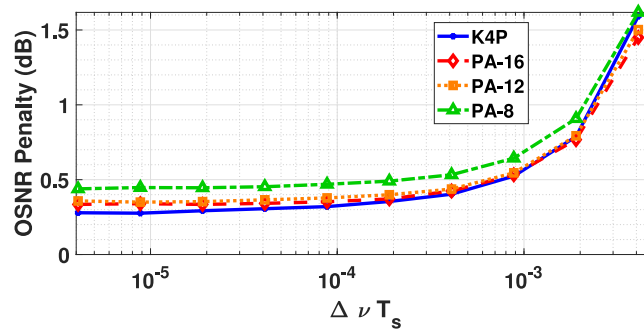


Fig. 4. Comparison of OSNR penalty incurred corresponding to a BER of 1×10^{-3} versus normalized linewidth for a 32 GBd 16QAM OFDM for proposed K4P algorithm and PA algorithm with 16, 12 and 8 pilots in back-back transmission.

sampled and processed using digital signal processing algorithms and its performance is evaluated. Numerical results for all the simulations performed for the single carrier transmissions is evaluated by using 42.2 million bits averaged over 100 realizations. The spectral efficiency (SE) calculated with the above mentioned parameters is as follows

$$SE(\text{bits/sec/Hz}) = \frac{N_{\text{filled}}}{N_{\text{FFT}} + N_{\text{CP}}} \times \frac{32 \text{ G}}{BW_{\text{Occupied}}} \times k, \quad (8)$$

where k is number of bits per QAM symbol.

4. Numerical Results & Discussion

4.1 B2B Performance

First, the optical B2B performance is studied by varying the normalized linewidth. For each linewidth, BER is evaluated as a function of OSNR after post-processing with both pilot aided and K4P algorithm. Fig. 4 shows the OSNR penalty for a BER of 1×10^{-3} . As the number of pilots increases, the corresponding OSNR penalty decreases as expected. It is evident that- for smaller values of $\Delta\nu T_s$, the OSNR penalty for the K4P algorithm is smaller than that by the PA technique. At a high normalized linewidth of 2×10^{-3} , the difference in penalty observed between the proposed K4P algorithm and the PA algorithm (with 16 pilots) for 16QAM CO-OFDM is less than 0.2 dB; but the K4P algorithm provides an improvement in spectral efficiency (SE) of $\approx 18\%$ when compared to the PA algorithm. The proposed algorithm performs better than the PA algorithm for up to 8 pilots: 0.05 dB lesser penalty and $\approx 8\%$ more SE. For a given modulation format, the performance of the proposed algorithm will remain the same even with different OFDM parameters as long as the normalized linewidth ($\Delta\nu T_s$) is retained.

4.2 Single Channel Fiber Transmission Performance

We now proceed to evaluate the performance of these algorithms in a fiber transmission link. The propagation of optical signal through the fiber is simulated by solving the nonlinear Schrodinger equation with split step Fourier method. The PDM-OFDM signal is transmitted through N_{SPAN} spans, each span consisting of 80 km long uncompensated SSMF (dispersion parameter of 17 ps/km.nm, nonlinear parameter of $1.4 \text{ W}^{-1} \text{ km}^{-1}$), with the attenuation (0.2 dB/km) which is completely compensated using an optical amplifier (noise figure = 5 dB) at the end of every span. The propagated optical signal is fed to the coherent receiver and the digital output is compensated for dispersion and CPE. In both K4P and PA methods, the signals in each polarization is assumed to have perfect frequency and timing synchronization (usually Schmidl-Cox based synchronization algorithm is used). Nonlinear effects play a critical role in deciding the reach and hence we first optimize the

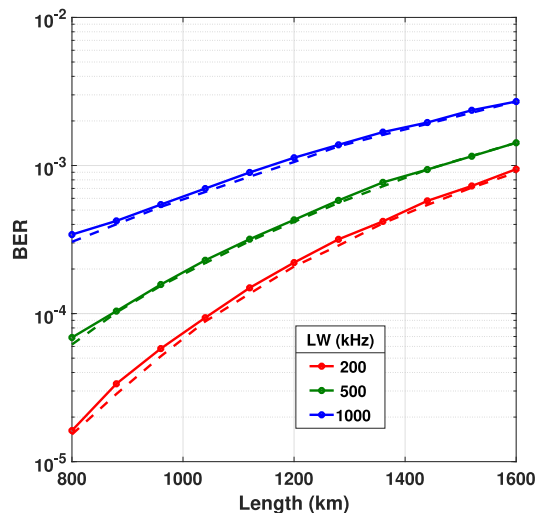


Fig. 5. BER performance comparison of the 32 GBd 16QAM OFDM for proposed K4P algorithm (continuous lines) with PA algorithm (dashed lines) with 12 pilots. The plots are for different transmitter and the receiver lasers linewidths: 100 KHz, 250 KHz and 500 KHz.

power launched into the fiber. We vary the launched power for a PDM-16QAM OFDM system and as expected, the performance improves with an increase in launched power upto the optimal launch power (found to be -1.5 dB for PA case and -2 dBm for K4P). Hence even though the input power launched can be higher for PA, the minimum BER achieved is the same as K4P.

Fig. 5 depicts the BER performance of 32 GBd PM-16QAM CO-OFDM transmission of 200 Gbps net information rate over 10 (800 km) to 20 (1600 km) spans of fiber with a launched power of -1.5 dBm and -2 dBm for K4P and PA-12 (PA with 12 pilots, 12 pilots are chosen to have a better CPE estimate) algorithms respectively and for various linewidth values. For the desired pre-FEC BER of 1×10^{-3} , we observe that almost same reach is achieved for both pilot aided and the blind algorithm cases with an improvement in spectral efficiency of $\approx 18\%$ for the K4P case.

4.3 Multi Channel Fiber Transmission Performance

We now proceed to evaluate the performance of multichannel CO-OFDM transmission. A flexi-grid based five WDM lines at 37.5 GHz spacing is chosen with central carrier at 1550 nm. For each optical carrier, a 32 GBd 16QAM OFDM signal is generated with the parameters as discussed for a single optical carrier transmission. The generated data is then modulated onto the comb of optical carriers, centered at 1550 nm (each of linewidth $= \frac{\Delta\nu}{2}$), using an IQ modulator. The net information data rate of the signal is 1 Tbps. The modulated spectrum in x-polarization is shown in Fig. 6, similar spectrum is observed for the y-polarization data. The propagation of multi-channel optical signal through the fiber is simulated by solving the nonlinear Schrodinger equation with split step Fourier method. The PDM-OFDM signal is transmitted over N_{SPAN} spans with amplifiers compensating for the loss in each span. The received optical signal is first filtered to choose the desired signal band and is fed to the coherent receiver and the digital output is processed using DSP algorithms for dispersion and CPE compensation (PA or K4P algorithm). As in the single-channel case, the signal is assumed to have perfect frequency and timing synchronization in each polarization for both K4P and PA cases. As in case of single channel, we first optimize the power launched into the fiber; Fig. 7(a) shows the BER evaluated as a function of launched power for a distance of 1600 km. The solid lines show the results from K4P algorithm and the dotted line shows the results of PA-12 algorithm and as expected, the performance is found to improve with an increase in launched power upto the optimal launch power (found to be ≈ 4.5 dBm for PA case and 4 dBm for K4P). The BER performance degrades beyond a certain optical launched power as expected, because of nonlinear

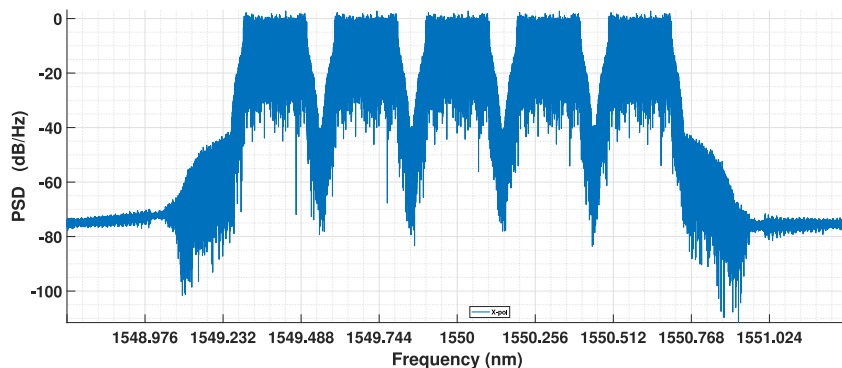


Fig. 6. Spectrum of multi-channel data generated in X-polarization with channel spacing of 0.3 nm.

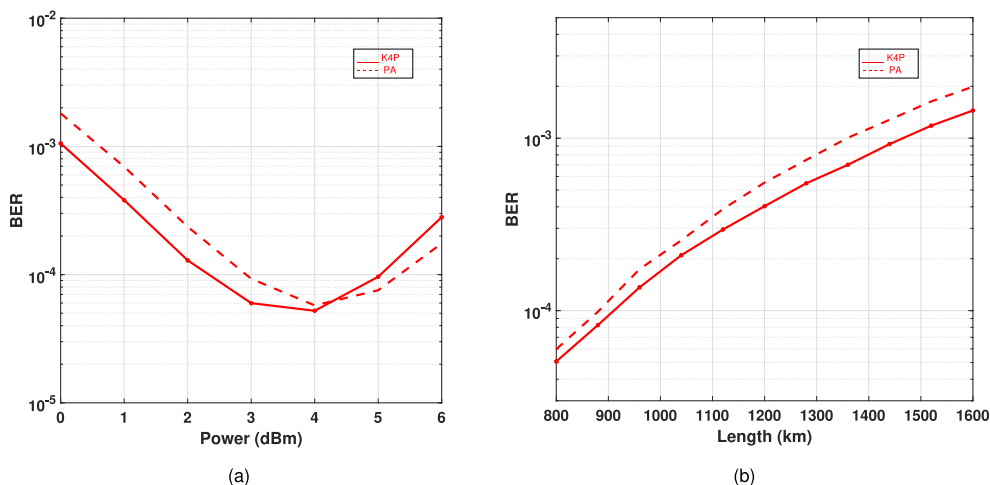


Fig. 7. (a) Launched power optimization performed for 5 channel 16QAM CO-OFDM transmission for a combined laser linewidth of 200 kHz for PA (dashed line) and K4P (continuous line) algorithms. (b) BER performance (averaged over all channels) of 5 channel 16QAM CO-OFDM transmission for a combined laser linewidth of 200 kHz for PA (dashed line) and K4P (continuous line) algorithms over SSMF.

effects in the fiber. The nonlinear threshold for the pilot aided case is found to be larger and the penalties induced due to nonlinear effects is relatively smaller because of relatively smaller power per subcarrier. The performance of K4P is better in the linear regime and is attributed to the relatively higher power per subcarrier. Fig. 7(b) depicts the average BER performance of multi channel 32 GBd PM-16QAM CO-OFDM transmission of 1 Tbps net information rate over 10 to 20 spans of fiber with a launch power of -1.5 dBm and -2 dBm for K4P and PA-12 algorithms respectively and for a combined laser linewidth of 200 kHz. For the desired pre-FEC BER of 1×10^{-3} , we observe that about ≈ 100 km reach extension is observed for the K4P algorithm over the pilot aided algorithm. For a given symbol duration, 64QAM OFDM transmission is expected to use a laser of linewidth twenty times narrower, for achieving the same performance as that of 16QAM OFDM [12]. Hence for a given linewidth higher order QAM would require more number of pilot subcarriers for better estimation of common phase error. For a five optical carrier super channel single polarization CO-OFDM system with $128 N_{FFT}$ and $8 N_{CP}$ points and at a baseband sampling rate of 32 GS/s, if we could replace pilot subcarriers with data subcarriers, we can achieve enhanced data rates. To elucidate with an example, for instance, considering a super channel with 5 optical carriers of 64QAM transmission with per-carrier bandwidth occupancy of 30 GHz and 12 pilot subcarriers, the actual information rate is only 1.62 Tbps. If we could replace the pilot subcarrier with data subcarriers, the net information rate will now be increased to 1.8 Tbps (increment of 180 Gbps, which is very significant).

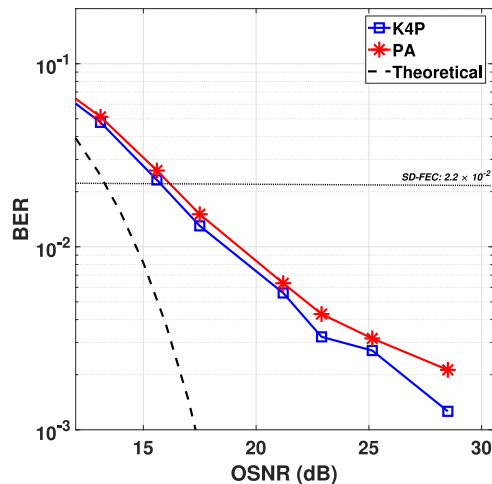


Fig. 8. BER Vs OSNR performance of 120 Gbps 16QAM CO-OFDM transmission for both PA and proposed K4P algorithms.

5. Experimental Results & Discussion

The schematic of the experimental setup is shown in the Fig. 3. In the baseband offline signal generation at the transmitter, a pseudo random bit sequence (PRBS) of order 15 was mapped to 16QAM symbols. The serial data is then parallelized and the information in frequency domain (occupying total bandwidth of 30 GHz and with 8 symbol pilot addition) is transferred to time domain by performing 128 point IFFT operation. The generated complex OFDM symbol has reduced guard interval, that is only 8 samples cyclic prefix were added in this experiment. It is to be noted that the length of cyclic prefix is increased in the experiments to 8 compared to that of 3 in simulations. The increase was made in order to correct of any residual ISI in the system and hence there is a slight reduction in the SE as compared to simulations. This parallel data is then converted to serial data followed by clipping (with clipping ratio 4) to reduce the PAPR. Each frame of the data consists of 200 OFDM symbols, the I and Q data are loaded respectively a two-channel arbitrary wave form generator (AWG, 64 GSa/s), which generates the corresponding electrical waveforms. Optical continuous wave at 1550 nm ($\Delta\nu \approx 50$ kHz) is internally fed to an IQ transmitter (IQ Tx) consisting of a pair of intensity modulators and a phase modulator. The IQ Tx is driven by the amplified waveforms from the two channels of AWG at the rate of 32 GBaud. Noise loading for OSNR variation is performed by ASE injection to the generated CO-OFDM signal to emulate a long haul transmission. The signal is then amplified using an EDFA followed by an optical filter (1 nm bandwidth) to remove the out of band amplified spontaneous emission (ASE) noise. Pump in the pre-amplifier is set to have appropriate gain to provide a power of 3 dBm at the receiver. The polarization is adjusted to have maximum power coupled in one of the polarization and is then fed to a phase diverse coherent receiver with a local oscillator tuned to 1550 nm and with $\Delta\nu \approx 50$ KHz. The RF signal after the photo-detection is then fed to the real time scope (RTS) (80 GS/s) and the digitized data is used for further processing.

In the post processing, the captured data was first corrected for frequency offset using the periodogram technique [13] and then re-sampled from 80 GSa/s to 64 GSa/s. The resampled data sequence is then correlated with one frame of the transmitted OFDM symbol. One frame in each data set is parallelized and converted from time domain to frequency domain by performing N_{FFT} -point FFT operation. Channel estimation is performed using the first ten symbols of both transmitted and received frame. Channel equalization was performed in the frequency domain information symbols and are then mapped back to bit sequences and BER as performance evaluation metric is calculated. The electrical bandwidth at the receiver was chosen to be 25 GHz. Fig. 8 shows the BER performance of the 16QAM coherent OFDM data at 32 GBd symbol rate of transmission. For each

OSNR, BER measurement is averaged over about 9×10^6 bits. A standard SD-FEC of 2×10^{-2} is also plotted for reference. It is observed that both the PA and K4P algorithm's performances are similar. We observe an increase in penalty as OSNR increases and it is attributed to our system penalty. With the use of K4P algorithm, about 2 GHz of bandwidth can be reallocated for the transmission of data instead of the pilots there by increasing the spectral efficiency by about 6.25%. This algorithm can be further extended by modifying and incorporating equalization for the effect of ICI and the state vector of the Kalman filter can also take additional parameter to estimate and correct the residual frequency offset, if any.

6. Conclusion

We propose a novel blind CPE estimation for any square MQAM CO-OFDM system using weighted QPSK partitioning to estimate the CPE and linear Kalman filter to predict and smooth the estimates. We have demonstrated the performance of proposed K4P algorithm against PA algorithm at various OSNR conditions- both through simulations and through experiments. We have also demonstrated the wide range phase noise adaptability of the proposed K4P algorithm as a function of OSNR penalty and since the OSNR penalty difference is within acceptable limits of 0.5 dB for 16QAM CO-OFDM, the pilots can be dropped to increase the power per sub-carrier and could potentially increase the reach of transmission. Using K4P algorithm, we have also demonstrated numerically that in long-haul Terabit/s superchannel transmission in linear regime based on PM-16QAM OFDM when $\Delta\nu T_s < 2 \times 10^{-3}$ we achieve a significant increment in reach and spectral efficiency per signal band. We have also experimentally demonstrated penalty-free transmission of 120 Gbps 16QAM CO-OFDM processed using the proposed pilot-free algorithm.

References

- [1] X. Chen, S. Chandrasekhar, P. Pupalais, and P. Winzer, "Fast DAC solutions for future high symbol rate systems," in *Proc. Opt. Fiber Commun. Conf. Exhib.*, Mar. 2017, pp. 1–3.
- [2] S. Chandrasekhar, X. Liu, B. Zhu, and D. W. Peckham, "Transmission of a 1.2-tb/s 24-carrier no-guard-interval coherent OFDM superchannel over 7200-km of ultra-large-area fiber," in *Proc. 35th Eur. Conf. Opt. Commun.*, Sep. 2009, pp. 1–2.
- [3] F. Buchali, R. Dischler, and X. Liu, "Optical OFDM: A promising high-speed optical transport technology," *Bell Labs Tech. J.*, vol. 14, no. 1, pp. 125–146, Spring 2009.
- [4] S. Wu and Y. Bar-Ness, "OFDM systems in the presence of phase noise: Consequences and solutions," *IEEE Trans. Commun.*, vol. 52, no. 11, pp. 1988–1996, Nov. 2004.
- [5] X. Yi, W. Shieh, and Y. Tang, "Phase estimation for coherent optical OFDM transmission," in *Proc. COIN-ACOFT, Joint Int. Conf. Opt. Internet 32nd Australian Conf. Opt. Fibre Technol.*, Jun. 2007, pp. 1–3.
- [6] M. E. M. Pasandi and D. V. Plant, "Improvement of phase noise compensation for coherent optical OFDM via data-aided phase equalizer," in *Proc. Conf. Opt. Fiber Commun., Collocated Nat. Fiber Optic Engineers Conf.*, Mar. 2010, pp. 1–3.
- [7] M. E. Mousa-Pasandi and D. V. Plant, "Zero-overhead phase noise compensation via decision-directed phase equalizer for coherent optical OFDM," *Opt. Exp.*, vol. 18, no. 20, pp. 20651–20660, Sep. 2010. [Online]. Available: <http://www.opticsexpress.org/abstract.cfm?URI=oe-18-20-20651>
- [8] Y. Ha and W. Chung, "Non-data-aided phase noise suppression scheme for CO-OFDM systems," *IEEE Photon. Technol. Lett.*, vol. 25, no. 17, pp. 1703–1706, Sep. 2013.
- [9] T. T. Nguyen, S. T. Le, M. Wuilpart, T. Yakusheva, and P. M egret, "Simplified extended Kalman filter phase noise estimation for CO-OFDM transmissions," *Opt. Exp.*, vol. 25, no. 22, pp. 27 247–27 261, Oct. 2017. [Online]. Available: <http://www.opticsexpress.org/abstract.cfm?URI=oe-25-22-27247>
- [10] I. Fatadin, D. Ives, and S. J. Savory, "Carrier phase recovery for 16-qam using QPSK partitioning and sliding window averaging," *IEEE Photon. Technol. Lett.*, vol. 26, no. 9, pp. 854–857, May 2014.
- [11] B. Szafraniec, T. Marshall, and D. M. Baney, "Kalman filtering for optical impairment estimation and compensation," in *Proc. Opt. Soc. Amer.*, 2015, Art. no. SpT4D.1. [Online]. Available: <http://www.osapublishing.org/abstract.cfm?URI=SPPCom-2015-SpT4D.1>
- [12] W. Shieh and I. Djordjevic, "Chapter 8-spectrally efficient high-speed coherent OFDM system," in *OFDM for Optical Communications*, W. Shieh and I. Djordjevic, Eds. Oxford, U.K.: Academic, 2010, pp. 295–323. [Online]. Available: <http://www.sciencedirect.com/science/article/pii/B9780123748799000083>
- [13] Y. Gao, Q. Zhuge, D. V. Plant, C. Lu, and A. P. tao Lau, "Blind and universal DSP for arbitrary modulation formats and time domain hybrid QAM transmissions," in *Proc. Opt. Fiber Commun. Conf.*, 2014, Art. no. Th3E.5. [Online]. Available: <http://www.opticsinfobase.org/abstract.cfm?URI=OFC-2014-Th3E.5>